SYNCHROTRON RADIATION

R.P. Walker
Sincrotrone Trieste, Italy

Abstract
The basic properties of synchrotron radiation are described, and their relevance to the design of electron and proton rings is discussed. The development of specialized sources of synchrotron radiation is also considered.

1. INTRODUCTION

The electromagnetic radiation emitted by a charged particle beam in a circular accelerator is termed "synchrotron radiation" (SR) after its first visual observation nearly 50 years ago in the General Electric (G.E.) 70 MeV Synchrotron. The theoretical basis for understanding synchrotron radiation however goes back much further. Maxwell's equations (1873) made it clear that changing charge densities would radiate electromagnetic waves, and Hertz demonstrated these waves in 1887. The first more directly relevant development was the publication of Liénard's paper entitled "The electric and magnetic field produced by an electric charge concentrated at a point and in arbitrary motion" [1]. This work includes the energy loss formula for particles travelling on a circular path with relativistic velocities. Later, Schott published a detailed essay that included also the angular and frequency distribution of the radiation, as well as the polarization properties [2].

No further interest appears to have been taken in the topic until the early 1940's, when theoretical work in the Soviet Union showed that the energy loss may pose a limit on the maximum energy obtainable in the betatron [3]. Then in 1946 Blewett measured the energy loss due to SR in the G.E. 100 MeV betatron and found agreement with theory, but failed to detect the radiation after searching in the microwave region of the spectrum [4]. It was later pointed out by Schwinger however that the spectrum peaks at a much higher harmonic of the orbit frequency and that the power in the microwave region is negligible [5]. The first direct observation of the radiation as a "small spot of brilliant white light" occured by chance in the following year at the G.E. 70 MeV synchrotron, when a technician was looking into the transparent vacuum chamber [6]. Later accounts of the event may be found in Refs. [7,8].

Soon after the discovery of SR the first systematic studies of the spectral distribution of the radiation were carried out in the visible part of the spectrum [9]. The results showed agreement with theory, which had been re-derived by Schwinger and expressed in a convenient form for practical computation [10]. At the 300 MeV synchrotron at Cornell experiments were carried out which accurately confirmed that the energy loss rate was proportional to the fourth power of electron energy, in agreement with theory [11]. Later, detailed spectral measurements were carried out in the UV and soft X-ray region by Tomboulian and Hartman [12]. Agreement between theory and measurement was also reported in the work carried out at the synchrotron of the Lebedev Institute, Moscow [13].

The emission of synchrotron radiation exerts a strong influence on the electron beam dynamics. It was already known before the first observation of SR that the energy loss would lead to a damping of the energy or synchrotron oscillations, a process known as Radiation Damping [14–16]. It was subsequently discovered, firstly by means of a quantum mechanical treatment [17] and later by a classical approach [18], that quantum fluctuations in the emission would give rise to a growth of oscillation amplitude and that the combined effect of the two processes would lead to a stable equilibrium [18]. Soon after, the same processes were found to occur also for the betatron oscillations [19,20]. Experimental verification of these effects was carried out at the synchrotron of the Lebedev Institute, Moscow [21].

Synchrotron radiation is of major importance in the design of electron synchrotrons and storage rings. The energy loss strongly affects the size of accelerator needed to reach a given energy. The design of the magnet lattice affects the processes of radiation damping and quantum excitation, and determines whether an equilibrium can be reached and the magnitude of the resulting beam dimensions. The emission of SR also has important implications for the design of ring components. A powerful r.f. system is needed to replace the energy lost due to SR. The design of the vacuum system must take into account the heat generated and the large amount of gas desorbed when SR beams impinge on the vacuum chamber walls. At high energies it becomes necessary to shield the vacuum chamber to prevent high energy photons escaping into the air and causing damage to other accelerator components. On the positive side, SR is widely used as a sensitive means of observing the electron beam.

Synchrotron radiation is also of major importance as a source of radiation for experiments. Following the work at Cornell in the early 50's it was pointed out that SR would be a useful source both for absorbtion measurements and as a standard for calibrating detectors in the VUV (vacuum ultra-violet) region of the spectrum [12]. Subsequently, in the early 1960's, several SR facilities were set up on rings built initially for High Energy Physics, in the U.S.A, Japan and in Europe. So successful was this "parasitic" use of the SR that a second generation of storage rings were built, for dedicated use as synchrotron radiation sources. At present a third generation of more sophisticated rings are under construction, and further developments are likely to continue.

In this Chapter the basic properties of synchrotron radiation and the way it affects the design of electron rings are described. Subsequent Chapters consider in more detail the effect of SR on beam dynamics. The development of specialized SR sources is treated briefly in Section 6. SR is emitted by any accelerated charge, but until recently particle energies have been sufficiently low that the effects have needed to be considered only in the case of electrons. For the next generation of high energy proton machines however the effects of SR emission will become significant. Although the treatment in this and subsequent chapters will be directed to the most common case, i.e. electrons, the formulae presented are valid for both electrons and protons unless indicated otherwise. Some special aspects of SR emission in proton rings are considered in Section 7.

2. BASIC PROPERTIES

2.1 Radiated power

The instantaneous power radiated by a moving electron, valid in the relativistic case, is given by the Liénard formula:

$$P = \frac{2}{3}\frac{e^2}{4\pi\varepsilon_0 c}\gamma^6\left[\dot{\boldsymbol{\beta}}^2 - \left(\boldsymbol{\beta}\wedge\dot{\boldsymbol{\beta}}\right)^2\right] \tag{1}$$

where βc is the velocity and $\gamma\,((1-\beta^2)^{-1/2})$ is the usual relativistic factor. The result is most easily derived by a Lorentz transformation of the result for a non-relativistic electron [22], obtained by Larmor:

$$P = \frac{2}{3}\frac{e^2}{4\pi\varepsilon_0 c}\frac{\dot{v}^2}{c^2} \tag{2}$$

We consider first the case of *linear motion*, for which $\boldsymbol{\beta}\wedge\boldsymbol{\beta} = 0$. In this case it can be shown that:

$$P = \frac{2}{3}\frac{e^2}{4\pi\varepsilon_0 m^2 c^3}\left(\frac{dp}{dt}\right)^2 \tag{3}$$

where $\boldsymbol{p}$ is the relativistic momentum ($\gamma\beta mc$). Since the rate of change of momentum ($d\boldsymbol{p}/dt$) is equal to the gain in energy per unit distance (dE/ds), we can write the ratio of the rate of energy loss to the rate of energy gain as follows:

$$\frac{2}{3}\frac{e^2}{4\pi\varepsilon_0 m^2 c^4}\left(\frac{dE}{ds}\right) = \frac{2}{3}\frac{r_0}{mc^2}\frac{dE}{ds} \tag{4}$$

Thus, unless the rate of energy gain is comparable to the rest mass energy (0.511 MeV) in a distance equal to the classical electron radius ($2.8\ 10^{-15}$ m) the radiative energy loss is negligible. As a further demonstration of this fact, it can be calculated that the energy loss in a typical 2 GeV linac, 200 m long, is only $7\ 10^{-5}$ eV.

In the case of *circular motion*, we have $\boldsymbol{\beta} \wedge \boldsymbol{\beta} = \beta\ \dot{\beta}$. In this case it may be shown that:

$$P = \frac{2}{3}\frac{e^2}{4\pi\varepsilon_0 m^2 c^3}\gamma^2\left(\frac{d\boldsymbol{p}}{dt}\right)^2 \tag{5}$$

Thus, for the same applied force ($d\boldsymbol{p}/dt$) the power radiated is a factor of γ^2 larger than for linear motion; moreover, it should be remembered that a given force is much more easily generated with a magnetic field compared to an electric field: a field of 1 Tesla produces the same force as an electric field of 300 MV/m.

For circular motion we have from the above that the instantaneous rate of power emitted is:

$$P = \frac{2}{3}\frac{e^2 c}{4\pi\varepsilon_0}\frac{\beta^4\gamma^4}{\rho^2} \tag{6}$$

Evaluating this expression we find that the resulting instantaneous power is apparently very small - only 7 μW even in the case of LEP at 100 GeV. A more directly meaningful parameter is the total energy loss per turn:

$$U_0 = \oint \frac{P}{\beta c} ds = \frac{2}{3}\frac{e^2}{4\pi\varepsilon_0}\beta^3\gamma^4 \oint \frac{ds}{\rho^2} \tag{7}$$

For an isomagnetic lattice (uniform bending radius in the bending magnets) the result simplifies to:

$$U_0 = \frac{e^2}{3\varepsilon_0}\frac{\beta^3\gamma^4}{\rho} \tag{8}$$

In practical units, for electrons:

$$U_0\ [\text{eV}] \;=\; 8.85\ 10^4\ \frac{E^4\ [\text{GeV}]}{\rho\ [\text{m}]} \;=\; 2.65\ 10^4\ E^3[\text{GeV}]\ B\ [\text{T}] \tag{9}$$

Since an accelerating voltage at least as great as the energy loss per turn is required for the electron to be stable it can be seen from the examples in Table 1 that this can be an appreciable quantity. For a beam of electrons the total power emitted can be obtained as follows:

$$P_b = \frac{U_0 N_e}{T_0} = \frac{U_0 I_b}{e} \qquad (10)$$

where N_e is the number of electrons in the ring, T_0 the orbit time, and I_b the average beam current. In practical units therefore the total power (in Watts) is simply the energy loss per turn (in eV) multiplied by the beam current (in Amps). With beam currents in the few mA to few 100 mA range it can be seen that the total SR power can be very large. This is also the power that the r.f. system must provide to make up for the losses due to SR emission.

It can be seen that there is a rapid increase in SR emission with energy, varying as E^4. There is therefore also a strong dependence on the mass of the particle, $\sim 1/m^4$, and so for protons with the same energy and bending radius the quantities are reduced by a large factor, $\sim 10^{13}$, compared to electrons.

Table 1
Energy loss per turn (U_0 and critical energy (ε_c) in various electron storage rings

Ring	E [GeV]	ρ [m]	U_0 [MeV]	ε_c [keV]
EPA	0.6	1.43	0.008	0.34
SRS	2.0	5.6	0.25	3.2
DORIS	5.0	12.3	4.5	22.5
PEP	18	166	56.1	78.1
HERA	30	550	140	109
LEP	55	3100	261	119
	100	3100	2855	715

2.2 Qualitative description of angular and spectral properties

Consider an electron travelling with speed βc along a circular path with constant radius ρ in a bending magnet (Fig. 1a). Viewed in a frame moving with the same speed in a direction tangent to the curve at some point P, the motion appears as shown in Fig. 1b. There is clearly an acceleration of the electron in the x' direction which gives rise to the emission of radiation. Since the motion in this frame is non-relativistic the radiation pattern is that of the familiar dipole radiation with $\sin^2\theta$ distribution, where θ is the angle with respect to the acceleration (x') axis [22]. Transformation of this distribution into the laboratory frame results in a distribution which is strongly peaked in the forward direction. This is evident from the fact that the angle at which zero emission occurs (x' axis, $\theta = 0$) transforms to an angle $1/\gamma$ in the laboratory frame (Fig. 1c), which can be a very small angle, e.g. 1/10 mrad for 5 GeV electrons.

The compression of the radiation into a narrow range of angles has an important consequence for the spectrum of the radiation. The radiation received in a given direction corresponds to only a small arc of the electron trajectory, of length $2\rho/\gamma$ (see Fig. 2). The radiation pulse length is the difference between the time it takes for the electron to travel around the arc from A to B (t_e) and the time for the photons to travel directly from A to B (t_υ). The radiation pulse length is then:

$$\Delta t = t_e - t_\upsilon = \frac{2\rho}{\gamma\beta c} - \frac{2\rho \sin(1/\gamma)}{c} \approx \frac{\rho}{\gamma^3 c} \qquad (11)$$

The short time interval implies a wide frequency range with typical frequency given approximately by $\omega \sim 1/\Delta t \sim \gamma^3 c/\rho$. In terms of the electron revolution frequency ($\omega_{rev} \approx c/\rho$) we see that $\omega/\omega_{rev} \sim \gamma^3$. The spectrum therefore extends to very much higher frequencies than the orbit frequency.

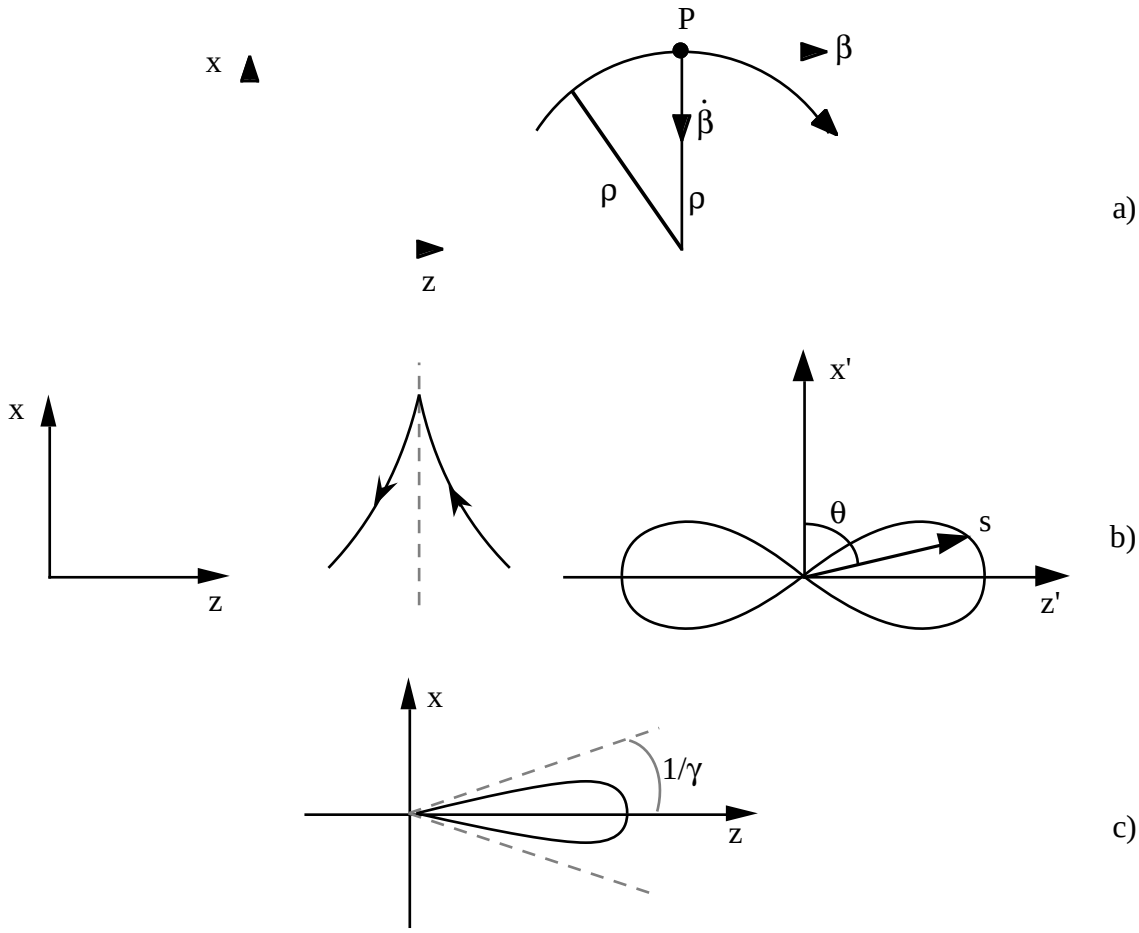

Fig. 1 Circular particle motion (a), the trajectory and dipole radiation emission pattern as seen in a frame moving with the average electron speed $\beta\, c$(b) and the corresponding radiation pattern transformed into the lab. frame (c).

As an example, if we take the parameters of the G.E. synchrotron (E = 70 MeV, ρ = 29.2 cm) we obtain a typical wavelength of about 7000 Å, i.e. in the visible part of the spectrum. It is evident also that with higher electron energies, ≥ 1 GeV, the emission will extend into the X-ray region.

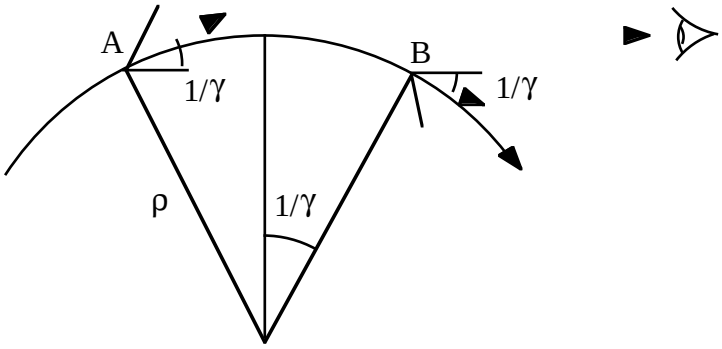

Fig. 2 Illustration of the limited arc of the trajectory which contributes to the radiation seen by an observer in a given direction

3. SPECTRAL AND ANGULAR PROPERTIES

A complete calculation of the spectral and angular distributions of the radiation is somewhat lengthy and therefore beyond the scope of this introduction and so here we only sketch the main features of the calculation and present the most important results. Further details may be obtained from various reports and textbooks [22–27].

3.1 Observer and emitter time

For charges in relativistic motion a fundamental concept is the distinction between observer and emitter (or "retarded") time. An electron at position **r** at time t' emits radiation towards an observer at a distance $R(t')$ away in a direction defined by the unit vector $\mathbf{n}(t')$, see Fig. 3. The radiation arrives at the observer at a later time t, where:

$$t = t' + \frac{R(t')}{c} \tag{12}$$

Although this relation between the two times appears relatively simple, the fact that the distance R is changing with t' complicates the analysis significantly. Taking the derivative of the above it can be shown that:

$$\frac{dt}{dt'} = 1 - \mathbf{n} \cdot \beta = 1 - \beta \cos \theta \tag{13}$$

Thus, when the direction of motion (β) is pointing close to the direction of the observer ($\mathbf{n}$) we see that a time interval for the emitter (dt') is seen as a much shorter time interval (dt) for the observer:

$$\frac{dt}{dt'} \simeq \frac{1}{2}\left(\frac{1}{\gamma^2} + \theta^2\right) \tag{14}$$

This is another description of the compression of the pulse length, with its consequent effect on the radiation spectrum, that was discussed in section 2.2. It also explains why the radiated intensity is very much greater for relativistic particles. The intensity of the radiation per unit solid angle at the observer can be related to the square of the *apparent* acceleration of the particle, i.e. the acceleration seen in the time frame of the observer, which is therefore increased by a large factor due to the time compression effect [27].

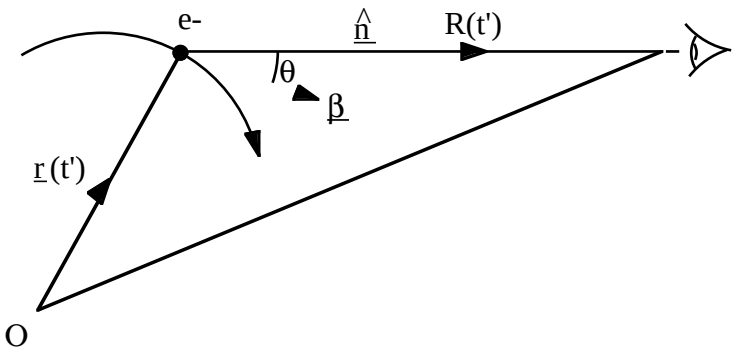

Fig. 3 Geometry of the emission of synchrotron radiation from a charged particle in arbitrary motion

3.2 Potentials and fields of a moving charge

The scalar electric and magnetic vector potentials of a slowly moving charge are given by the standard expressions:

$$V = \frac{e}{4\pi\varepsilon_0 R} \qquad \boldsymbol{A} = \frac{e\boldsymbol{v}}{4\pi\varepsilon_0 R} \tag{15}$$

where R is the distance from the charge to the observer and $\boldsymbol{v}$ the charge velocity. In the case of a relativistically moving charge we must take into account that the potential created by the charge reaches the observer at a later time, according to Eq. (12). Charges moving towards the observer contribute for a longer time and therefore result in a larger potential [26]. It can be shown that the resulting expressions are similar, but includes the time correction factor Eq. (13):

$$V(t) = \frac{e}{4\pi\varepsilon_0}\left[\frac{1}{R(1-\boldsymbol{n}\cdot\boldsymbol{\beta})}\right]_{ret.} \qquad \boldsymbol{A}(t) = \frac{e}{4\pi\varepsilon_0}\left[\frac{\boldsymbol{v}}{R(1-\boldsymbol{n}\cdot\boldsymbol{\beta})}\right]_{ret.} \tag{16}$$

where $[\ ]_{ret.}$ means evaluated at the emitter, or retarded time t'.

The electric and magnetic fields can then be calculated by applying Maxwell's equations:

$$\boldsymbol{E} = -\nabla V - \mu_0 \frac{\partial \boldsymbol{A}}{\partial t} \qquad \boldsymbol{B} = \mu_0(\nabla \wedge \boldsymbol{A}) \tag{17}$$

The operation is not so straightforward however, since derivatives with respect to the observer's position involve changes in emitter time. The resulting expressions are given as follows:

$$\boldsymbol{E}(t) = \frac{e}{4\pi\varepsilon_0}\left[\frac{\boldsymbol{n}-\boldsymbol{\beta}}{(1-\boldsymbol{n}\cdot\boldsymbol{\beta})^3 R^2\gamma^2}\right]_{ret.} + \frac{e}{4\pi\varepsilon_0 c}\left[\frac{\boldsymbol{n}\wedge\{(\boldsymbol{n}-\boldsymbol{\beta})\wedge\dot{\boldsymbol{\beta}}\}}{(1-\boldsymbol{n}\cdot\boldsymbol{\beta})^3 R}\right]_{ret.} \tag{18}$$

$$\boldsymbol{B}(t) = \frac{\boldsymbol{n}\wedge\boldsymbol{E}}{c}$$

From the above expressions we note the following features:

- $\boldsymbol{E}$ and $\boldsymbol{B}$ are mutually perpendicular;
- for a static charge $\left(\boldsymbol{\beta} = \dot{\boldsymbol{\beta}} = 0\right)$ we recover Coulomb's Law $\boldsymbol{E} = e\,\boldsymbol{n} / 4\pi\varepsilon_0 R$;
- the first term is independent of acceleration and is proportional to $1/R^2$, and is therefore negligible at large distances; this is termed the "velocity field";
- the second term depends directly on the acceleration, and since it varies as $1/R$ dominates at large distances; this is called the "acceleration field" or the "far field".

The second term is therefore the one that we shall consider. For this term we see that $\boldsymbol{E}$ and $\boldsymbol{B}$ are perpendicular to $\boldsymbol{n}$.

3.3 Power distribution

The flow of energy is described by the Poynting vector, $\boldsymbol{S}$:

$$\boldsymbol{S} = \frac{1}{\mu_0}(\boldsymbol{E} \wedge \boldsymbol{B}) \tag{19}$$

which is the energy passing through a unit area in direction $\boldsymbol{S}$. The energy received per unit solid angle in direction $\boldsymbol{n}$ at distance R from the source is therefore:

$$\frac{dP}{d\Omega} = R^2(\boldsymbol{S}\cdot\boldsymbol{n}) = \frac{1}{\mu_0 c}(R\boldsymbol{E})^2 \tag{20}$$

To express this in terms of the energy radiated per unit time of the emitter, we must include the factor in Eq. (13):

$$\frac{dP}{d\Omega}(t') = \frac{dP}{d\Omega}\frac{dt}{dt'} = \frac{dP}{d\Omega}(1-\boldsymbol{n}\cdot\boldsymbol{\beta}) \tag{21}$$

Inserting the expression for the electric field, Eq. (18), gives the general result for the angular distribution of the instantaneous power radiated by the charge:

$$\frac{dP}{d\Omega}(t') = \frac{e^2}{(4\pi)^2\varepsilon_0 c}\frac{\left(\boldsymbol{n}\wedge\left\{(\boldsymbol{n}-\boldsymbol{\beta})\wedge\dot{\boldsymbol{\beta}}\right\}\right)^2}{(1-\boldsymbol{n}\cdot\boldsymbol{\beta})^5} \tag{22}$$

In the case of circular motion ($\boldsymbol{\beta} \perp \dot{\boldsymbol{\beta}}$) and in the relativistic case, the resulting distribution is given by:

$$\frac{dP}{d\Omega}(t') = \frac{e^2 c}{2\pi^2\varepsilon_0}\frac{\gamma^6}{\rho^2}\left(\frac{1+2\gamma^2\theta^2\left(1-2\cos^2\phi\right)+\gamma^4\theta^4}{\left(1+\gamma^2\theta^2\right)^5}\right) \tag{23}$$

(See Fig. 4). Thus, in agreement with the results of section 2, we see that the distribution is strongly peaked in the forward direction within a cone $1/\gamma$. In the non-relativistic limit the electric field, Eq. (18), reduces to:

$$\boldsymbol{E}(t) = \frac{e}{4\pi\varepsilon_0 c}\frac{\boldsymbol{n}\wedge\left(\boldsymbol{n}\wedge\dot{\boldsymbol{\beta}}\right)}{R} \tag{24}$$

and hence the power distribution becomes:

$$\frac{dP}{d\Omega} = \frac{e^2}{(4\pi)^2\varepsilon_0 c}\left(\boldsymbol{n}\wedge\left\{\boldsymbol{n}\wedge\dot{\boldsymbol{\beta}}\right\}\right)^2 = \frac{e^2}{4\pi^2\varepsilon_0 c}\dot{\beta}^2\sin^2\Theta \tag{25}$$

with Θ as the angle between the acceleration axis and the radiation direction. Figure 5 shows a comparison of the instantaneous power distribution in the two cases.

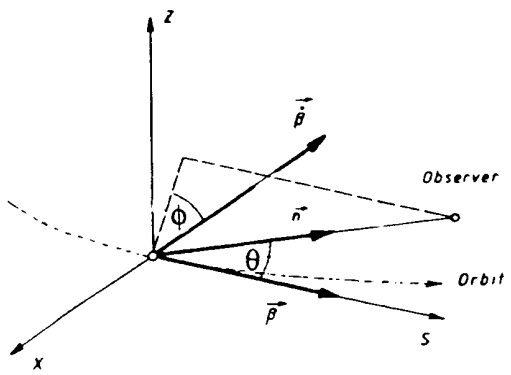

Fig. 4
Definition of angles θ and ϕ in the instantaneous radiation emission, Eq.(23)

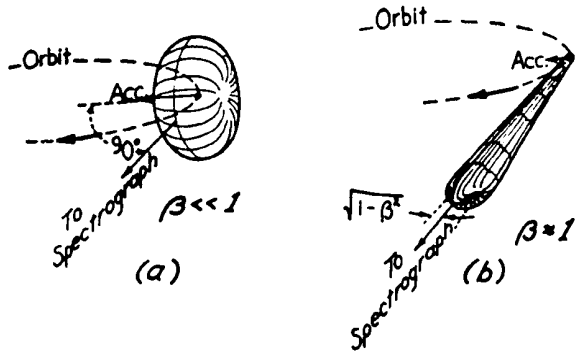

Fig. 5
Illustration of the instantaneous radiation pattern from a charged particle in a circular orbit in the non-relativistic (a) and the relativistic cases (b), from Ref.[12]

3.4 Spectral and angular distributions

In order to obtain the frequency dependence we define the Fourier transform of the electric field, $\tilde{\boldsymbol{E}}(\omega)$, and its inverse:

$$\tilde{\boldsymbol{E}}(\omega) = \frac{1}{\sqrt{2\pi}} \int_{-\infty}^{\infty} \boldsymbol{E}(t)\, e^{i\omega t}\, dt \qquad \tilde{\boldsymbol{E}}(t) = \frac{1}{\sqrt{2\pi}} \int_{-\infty}^{\infty} \tilde{\boldsymbol{E}}(\omega)\, e^{-i\omega t}\, d\omega \qquad (26)$$

The total energy received per unit solid angle during one passage of the electron past the observer is from Eq. (20):

$$\frac{dW}{d\Omega} = \int \frac{dP}{d\Omega}\, dt = \frac{1}{\mu_0 c} \int_{-\infty}^{\infty} (R\boldsymbol{E})^2\, dt \qquad (27)$$

Inserting the expression for the electric field and simplifying, results in the following integral over frequency:

$$\frac{dW}{d\Omega} = \frac{1}{\mu_0 c} \int_{0}^{\infty} 2 \left| R\tilde{\boldsymbol{E}}(\omega) \right|^2 d\omega \qquad (28)$$

The integrand in the above is therefore the required spectral and angular density. Inserting now the expression for $\boldsymbol{E}(\omega)$ we obtain finally:

$$\frac{d^2W}{d\omega d\Omega} = \frac{1}{2\pi\mu_0 c} \left| \int_{-\infty}^{\infty} (R\boldsymbol{E})\, e^{i\omega t}\, dt \right|^2 \qquad (29)$$

Thus, the total energy received per unit solid angle per unit frequency interval is the modulus-squared of the Fourier transform of the electric field seen by the observer.

Inserting the expression for the Electric field, Eq. (18), we obtain:

$$\frac{d^2W}{d\Omega d\omega} = \frac{e^2}{16\pi^3\varepsilon_0 c}\left|\int_{-\infty}^{\infty}\left[\frac{\boldsymbol{n}\wedge\left\{(\boldsymbol{n}-\boldsymbol{\beta})\wedge\dot{\boldsymbol{\beta}}\right\}}{(1-\boldsymbol{n}\cdot\boldsymbol{\beta})^3}\right]_{ret.} e^{i\omega t}dt\right|^2 \tag{30}$$

Thus, the general prescription for calculating the spectral/angular distribution for arbitrary electron motion is as follows: calculate the electron motion ($\boldsymbol{r}$, $\boldsymbol{\beta}$, $\dot{\boldsymbol{\beta}}$) and the direction and distance to the observer ($\boldsymbol{n}$, R) as a function of retarded (emitter) time, t'; calculate the electric field, Eq. (18); express as a function of observer time using $t = t' + R(t')/c$ and perform a Fourier transform. Alternatively, the integration can be expressed directly in terms of emitter time t':

$$\frac{d^2W}{d\Omega d\omega} = \frac{e^2}{16\pi^3\varepsilon_0 c}\left|\int_{-\infty}^{\infty}\frac{\boldsymbol{n}\wedge\left\{(\boldsymbol{n}-\boldsymbol{\beta})\wedge\dot{\boldsymbol{\beta}}\right\}}{(1-\boldsymbol{n}\cdot\boldsymbol{\beta})^2}\, e^{i\omega\left(t'+\frac{R(t')}{c}\right)}dt'\right|^2 \tag{31}$$

For circular motion the result can be derived analytically in terms of Airy integrals or alternatively modified Bessel functions:

$$\frac{d^2W}{d\Omega d\omega} = \frac{e^2}{16\pi^3\varepsilon_0 c}\,\gamma^2\left(\frac{\omega}{\omega_c}\right)^2\left(1+\gamma^2\psi^2\right)^2\left[K_{2/3}^2(\xi) + \frac{\gamma^2\psi^2}{1+\gamma^2\psi^2}\,K_{1/3}^2(\xi)\right] \tag{32}$$

where,

$$\xi = \frac{\omega}{\omega_c}\frac{\left(1+\gamma^2\psi^2\right)^{3/2}}{2} \tag{33}$$

Because of the horizontal motion of the source the result depends only on the observation angle in the vertical plane, ψ (Fig. 6). ω_c is the critical frequency defined by:

$$\omega_c = \frac{3}{2}\frac{\gamma^3 c}{\rho} \tag{34}$$

This is very similar to the value of the typical frequency derived earlier from consideration of the pulse length. Note that some authors use a value which is twice the above value [22]. Practical formulae for calculating the critical frequency are given in the Appendix.

The two terms in Eq. (32) above correspond to the radiation polarized in the horizontal (σ) and vertical (π) planes. The angular distributions at several different frequencies are shown in Fig. 7, for both polarization components, normalized in each case to the peak value on axis ($\psi = 0$). On axis the radiation is linearly polarized in the horizontal plane. As ψ increases the vertically polarized component increases, and because of a $\pi/2$ phase shift, not directly apparent from the intensities in Eq. (32) above, this results in circularly polarized radiation. The angular divergence changes markedly with the radiation frequency. At $\omega = \omega_c$, and approximating as a Gaussian function, the effective standard deviation is $0.57/\gamma$.

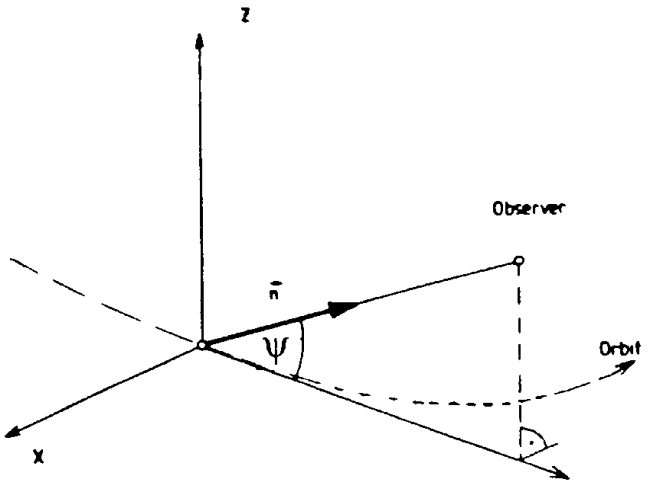

Fig. 6 Geometry of the emission of synchrotron radiation in the case of circular motion

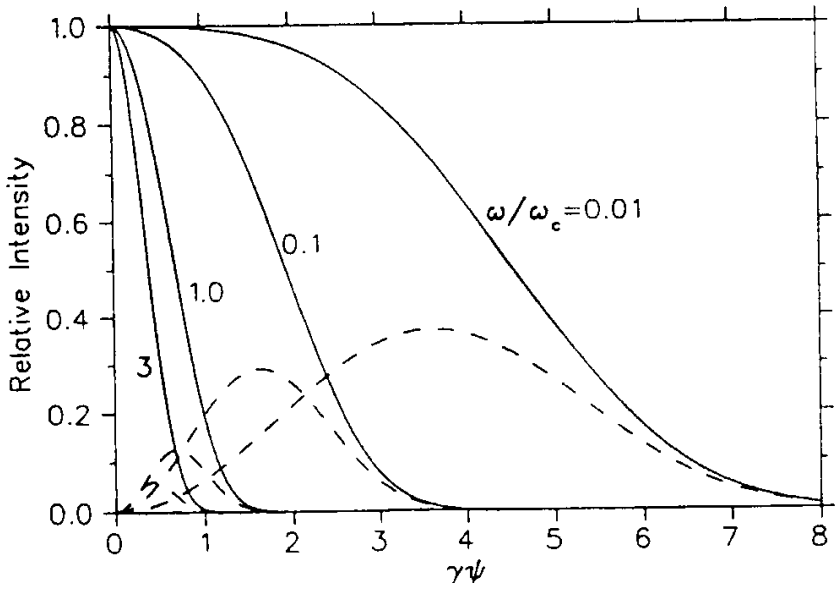

Fig. 7 Angular distribution of synchrotron radiation polarized in the orbit plane (solid lines) and in the plane perpendicular to the orbit plane (dotted lines)

The variation of the peak intensity on-axis as a function of frequency is given by:

$$\frac{d^2W}{d\Omega d\omega} = \frac{e^2}{16\pi^3\,\varepsilon_0\,c}\,\gamma^2\left(\frac{\omega}{\omega_c}\right)^2 K_{2/3}^2\left(\frac{\omega}{2\omega_c}\right) = \frac{e^2}{16\pi^3\,\varepsilon_0\,c}\,\gamma^2\,H_2\left(\frac{\omega}{\omega_c}\right) \qquad (35)$$

The function H_2 is shown in Fig. 8. As anticipated in section 2.2, it can be seen that the spectral range is very broad. The peak value occurs close to the critical frequency (ω/ω_c = 0.83) where H_2 has a value of 1.47.

Integrating Eq. (32) over all angles one obtains the energy radiated per unit frequency interval, per turn:

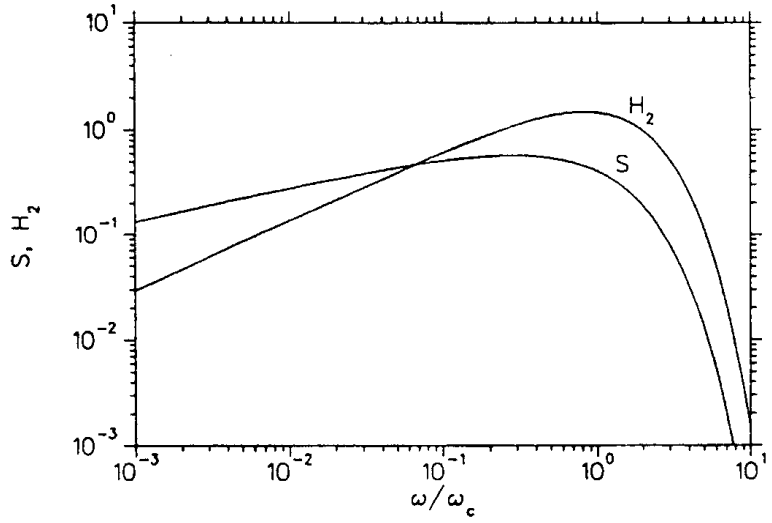

Fig. 8 Functions describing the spectral distributions of peak angular density (H_2) and intensity integrated over vertical angle (S)

$$\frac{dW}{d\omega} = \frac{\sqrt{3}\,e^2}{4\pi\varepsilon_0 c}\,\gamma\left(\omega/\omega_c\right)\int_{\omega/\omega_c}^{\infty} K_{5/3}\left(\omega/\omega_c\right)\,d\left(\omega/\omega_c\right) \tag{36}$$

This can be written as follows:

$$\frac{dW}{d\omega} = \frac{U_0}{\omega_c}S\left(\omega/\omega_c\right) \tag{37}$$

where $S\,(\omega/\omega_c)$ is the normalized spectrum, shown in Fig. 8, defined by:

$$S\left(\omega/\omega_c\right) = \frac{9\sqrt{3}}{8\pi}\,\frac{\omega}{\omega_c}\int_{\omega/\omega_c}^{\infty} K_{5/3}\left(\omega/\omega_c\right)\,d\left(\omega/\omega_c\right) \tag{38}$$

The spectrum is normalized since:

$$\int_0^{\infty} S\left(\omega/\omega_c\right)\;d\left(\omega/\omega_c\right) = 1 \tag{39}$$

It should be noted also that:

$$\int_0^{1} S\left(\omega/\omega_c\right)\;d\left(\omega/\omega_c\right) = 0.5 \tag{40}$$

In other words, half of the power is emitted above the critical frequency, and half below. The peak of the total spectrum occurs at $\omega/\omega_c = 0.29$ at which point $S = 0.57$. The spectrum of vertically integrated intensity is also often written in terms of the function $G_1\,(\omega/\omega_c)$ which includes all but the numerical factor in Eq. (38) and so the relation between the two is simply $S\,(\omega/\omega_c) = 0.620\;G_1\,(\omega/\omega_c)$.

Integrating over frequency one obtains the total energy radiated per unit solid angle (per pass):

$$\frac{dW}{d\Omega} = \frac{7e^2}{64\pi\varepsilon_0}\frac{\gamma^5}{\rho}\frac{1}{\left(1+\gamma^2\psi^2\right)^{5/2}}\left[1+\frac{5\gamma^2\psi^2}{7\left(1+\gamma^2\psi^2\right)}\right] \tag{41}$$

This distribution is shown in Fig. 9.

The Appendix includes practical versions of the above formulae.

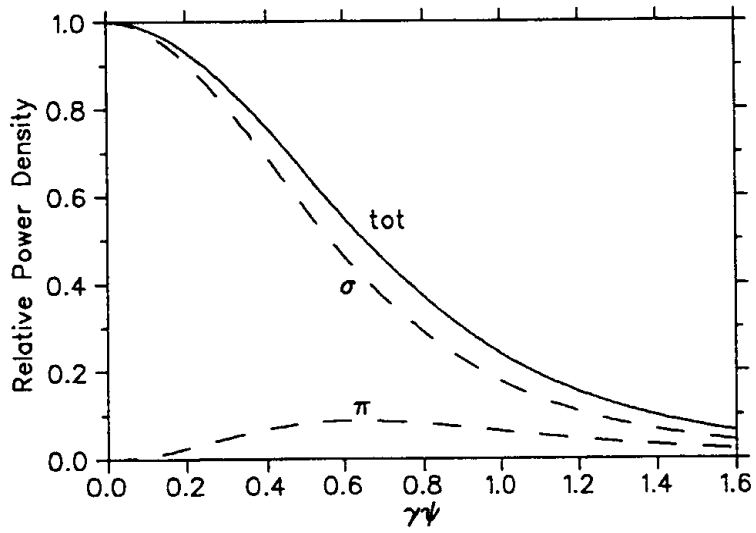

Fig. 9 Angular distribution of power density, polarized in the orbit plane (σ), in the plane perpendicular to the orbit (π), and total (tot).

4. PHOTON DISTRIBUTION

So far we have considered that an electron radiates energy continuously, which is an acceptable assumption from the point of view of calculating the spectral properties etc. In reality however, radiation is emitted in discrete 'quanta' or photons, each with an energy, u, given by:

$$u = \hbar\omega \tag{42}$$

where $\hbar$ = Planck's constant / 2π. The distribution of the number of photons emitted as a function of angle and frequency is of interest for a number of reasons. One of the effects on beam dynamics ("quantum excitation") depends directly on the number of photons emitted as a function of energy. Also, since individual photons desorb gas molecules, the effect on the vacuum system depends on the number of photons, not simply total power. In addition, the common unit of intensity employed by SR experimenters is the spectral flux – the number of photons per second per unit frequency. Expressions for this quantity are given in the Appendix.

For the effect on beam dynamics the important quantity is the instantaneous rate of emission of photons. We define a quantity $n(u)$, the number of photons per second radiated (on average) by a single electron per unit energy interval:

$$n(u)\Delta u = \frac{dW}{d\omega}\frac{c}{2\pi\rho}\frac{1}{\hbar\omega}\Delta\omega \tag{43}$$

hence,

$$n(u) = \frac{P}{u_c^2} \frac{S\left(u/u_c\right)}{\left(u/u_c\right)} \tag{44}$$

where,

$$u_c = \hbar\omega_c \tag{45}$$

The photon distribution function is shown in Fig. 10.

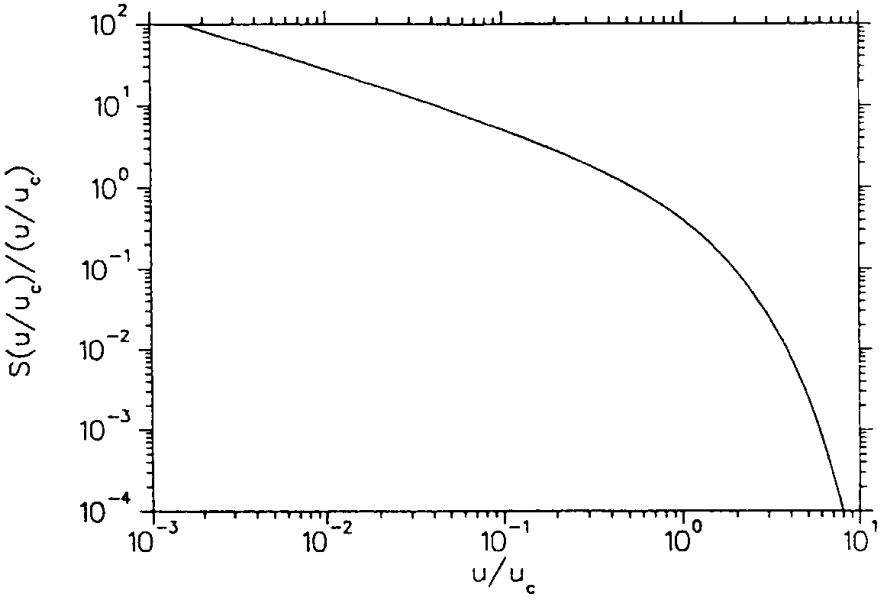

Fig. 10 Photon distribution function

The total number emitted (per electron per second) is then:

$$N = \int n(u)du = \frac{15\sqrt{3}}{8}\frac{P}{u_c} = \frac{5}{2\sqrt{3}}\frac{e^2}{4\pi\varepsilon_0\hbar}\frac{\gamma}{\rho} \tag{46}$$

From the above we can obtain the simple result that the number emitted per radian is:

$$N\frac{\rho}{c} = \frac{\gamma}{94.9} \tag{47}$$

which depends only on the energy, γ; similarly the number emitted per metre is:

$$\frac{N}{c} = 6.2\,B \qquad \text{(electrons)} \tag{48}$$

which depends only on the magnetic field strength. It can be appreciated that the number of photons emitted per electron is a small quantity, and will therefore be subject to large statistical fluctuations. This has an important consequence for the beam dynamics that will be treated in the Chapter on "Quantum Excitation".

For a beam of electrons, the total number of photons emitted is given by:

$$\frac{dF}{d\theta} = \frac{N\rho}{c}\frac{I_b}{e} = 1.3\ 10^{17}\ E\ [\text{GeV}]\ I_b\ [\text{A}] \qquad \text{photons/sec/mrad horizontal} \qquad (49)$$

In most cases therefore with average beam currents in the mA to several 100 mA range the total photon flux is large, with important consequences for the vacuum system (see section 5.2).

Two other expressions that will be of use in later Chapters are the mean and mean-square photon energy. The mean energy is:

$$\langle u \rangle = \frac{\int u\ \ n(u)du}{N} = \frac{P}{N} = \frac{8}{15\sqrt{3}}u_c \qquad (50)$$

which is related by a numerical factor to the critical energy. Similarly the mean-square energy is related to the square of the critical energy:

$$\left\langle u^2 \right\rangle = \frac{\int u^2\ \ n(u)du}{N} = \frac{8}{15\sqrt{3}}u_c^2 \int_0^\infty (u/u_c)S(u/u_c)d(u/u_c) = \frac{11}{27}u_c^2 \qquad (51)$$

5. SYNCHROTRON RADIATION ASPECTS IN ELECTRON ACCELERATOR DESIGN

5.1 R.f. requirements

To make up for the losses due to the emission of SR the r.f. system must provide a sufficient accelerating voltage and sufficient power. There is an additional voltage requirement above that of the energy loss per turn in order to maintain sufficient beam lifetime, as will be described in a later Chapter on "Quantum Excitation". The total power needed from the r.f. system must also take into account the significant losses in the walls of the accelerating cavity.

The very strong dependence of the energy loss with energy is a limiting factor in the construction of increasingly high energy circular electron accelerators. Some reduction in the r.f. requirement can be achieved by reducing the bending magnet field strength, but at the expense of a larger and therefore more costly machine. It can be seen from Fig. 11 that in electron storage rings built so far, parameter optimization has resulted in a bending radius that increases roughly as E^2 i.e. the field decreases as $1/E$. Thus the energy loss per turn, U_0, still increases as E^2. In LEP a field as low as 0.059 T is used at 55 GeV. Even so, 128 five-cell r.f. cavities are needed with sixteen 1 MW klystrons to power them [28]. To reach 100 GeV superconducting cavities will be used to reduce the power dissipated in the cavity. Because of the limitation imposed by SR emission attention is focussed on linear colliders for the next generation of high energy electron accelerators rather than circular machines.

As can be seen from Fig. 11, the situation is entirely different for proton machines. In this case SR emission is not a limiting factor and bending fields have increased by use of superconducting magnets.

5.2 Vacuum system

The power in the SR beams can be very high, up to several kW per metre of orbit length, and so water-cooled absorbers must be provided. The main gas load in the system is also caused by SR [29]: photons hitting the vacuum chamber produce photoelectrons which in turn desorb gas molecules from the surface. If the surface is clean before installation the main gas

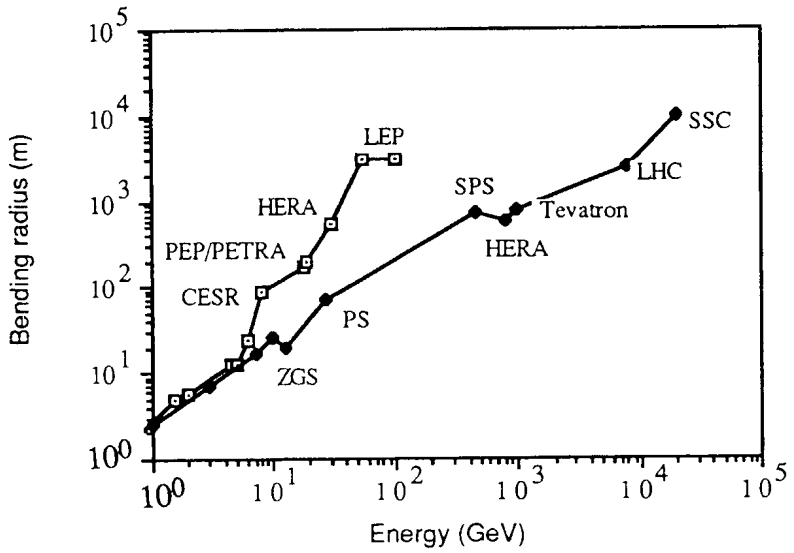

Fig. 11 Relationship between energy and bending radius for various circular electron and proton accelerators

molecules desorped are H_2, CO, CO_2 and CH_4. The consequence of this is that the gas pressure will increase, and hence the beam lifetime will decrease, when the beam current increases. However, the desorption decreases as a function of the total beam 'dose', as the SR cleans the vacuum chamber surface. Typically it is assumed in the design of the pumping system that a dose of about 50 Amp-hours is required before nominal pressure and lifetime is reached.

5.3 Radiation shielding

When the critical energy of the photons becomes sufficiently large, scattered high energy photons can escape from the standard type of aluminium or stainless steel vacuum chamber and cause radiation damage to ring components (e.g. magnet coils and water hoses), failures of electronic components, production of ozone and nitric oxide in the air, and in the presence of humidity corrosion of the vacuum chamber by nitric acid. Problems of this type were experienced first in PETRA [30] and TRISTAN [31] when energies were raised above 15 GeV, which required lead shielding to be added around the chambers. Later higher-energy machines took this into account at the start. In the HERA electron ring a copper-bronze alloy was used for the chamber, and use was made of the dipole magnet yokes as extra shielding [32]. The LEP vacuum chamber is surrounded by a lead shield between 3 and 8 mm thick [28].

5.4 Electron-beam diagnostics

SR is widely used to form visible images of the electron beam [33] both for direct observation and qualitative measurement of beam size, position, stability and also bunch length. A typical arrangement is to reflect the visible part of the SR emitted by a bending magnet off a water-cooled mirror, through the radiation shield wall and into a diagnostics area. By focussing the light with a lens onto a screen a direct image of the electron beam can be formed. Linear photodiode arrays or CCD matrices can be used to obtain accurate information on the beam profile and a position sensitive detector can provide information about the positional stability of the beam. Bunch length information can be obtained from streak cameras or fast photomultipliers [34].

In storage rings used as synchrotron radiation sources, the stability of the position and angle of the radiation source points is very important. For this reason monitors which determine the position of the SR in the beam-lines have been developed. Using signals from these detectors feedback systems can then be used to stabilize the electron beam orbit.

6. SYNCHROTRON RADIATION SOURCES

As many as 28 electron storage rings are currently used for research using SR, and of these 17 are fully dedicated to SR. In addition, 16 new dedicated rings are under construction or commissioning, and several more are under study [35]. Not included in this list are about 10 smaller rings built exclusively as sources for X-ray lithography.

The properties of SR that it make it so attractive as a research tool are as follows:

- high intensity or photon flux;
- continuous spectrum covering a broad range from the far infra-red to hard X-rays;
- small vertical angular divergence;
- small source size, determined mainly by the electron beam dimensions;
- high "brightness" and hence high partial coherence, resulting from the combination of small source size and divergence;
- polarization - linear in the orbit plane, with a circular component above and below the orbit plane;
- pulsed time structure, determined by that of the electron beam;
- calculable spectral intensity, allowing use as a calibrated source.

The wide range of applications cover the whole range of basic and applied science, and also include industrial (e.g. lithography and micro-mechanics) and medical (e.g. angiography) uses.

By convention the development of synchrotron radiation sources is usually described in terms of various "generations". The *first generation* includes synchrotrons and storage rings built initially for High Energy Physics and used "parasitically" for SR. The first experimental facilities for using SR were set up on the SURF and INS-SOR rings in 1963, followed by Frascati, DESY and Tantalus. Others followed, including the SPEAR ring (Stanford, USA), now dedicated to SR. The *second generation* rings are storage rings designed and built from the outset as dedicated SR sources. The first was the 300 MeV SOR-Ring in 1974, the first X-ray ring being the 2 GeV SRS (Daresbury, England). The *third generation* are newer dedicated rings with lower beam emittance (i.e. smaller beam sizes and divergences), and with many long straight sections into which special "insertion devices" (see below) can be placed. Third generation rings fall into three categories, according to the spectral region that they have been optimized for. Apart from one operating 0.8 GeV UV/VUV ring (SUPERACO, Orsay, France) the rest are either 1.2-2.0 GeV VUV/Soft X-ray rings or 6.0-8.0 GeV Soft/Hard X-rays rings.

The insertion devices that will form the main radiation sources in the third generation rings are magnetic devices with a field polarity that alternates along the electron beam trajectory [36]. A periodic deflection of the electron beam is produced, resulting in the emission of radiation with special properties that depend on the form of the magnetic field distribution. Compared to conventional bending magnet sources of SR, insertion devices can produce:

- higher photon energies;
- increased flux;
- increased brightness;
- different polarization characteristics.

Higher photon energies can be produced if the insertion device field, and hence critical photon energy, is larger than that of the bending magnets. If the device has a single high field pole, then it is often termed a *wavelength shifter*. The first such device was tested in the 240 MeV TANTALUS ring [37]. Several superconducting wavelength shifters are now operating with peak fields of 5-6 T. If the device has several magnet poles, then the output flux and brightness are increased accordingly and the device is generally called a *multipole wiggler*. If the parameters are such that interference effects are important, then very high brightness can be produced with a line, rather than continuous, spectrum; in this case the device is usually termed

an *undulator*. In the standard case where the insertion device deflects the particle in the horizontal plane the radiation is linearly polarized. Different polarization characteristics can be produced with more complicated helical, elliptical or non-sinusoidal electron trajectories [38].

Some aspects related to the design of third generation radiation sources and the effects of insertion devices on electron beam properties are considered in the Chapter on Quantum Excitation. Further details may be found in the Proceedings of a special CERN Accelerator School on Synchrotron Radiation Sources and Free Electron Lasers, Ref. [26].

7. SYNCHROTRON RADIATION FROM PROTONS

7.1 High energy proton rings

The equations governing the emission of Synchrotron Radiation are the same for both protons and electrons, however the total power radiated is inversely proportional to the 4th power of the rest mass, while the critical frequency of the spectrum varies as the inverse of the mass to the 3rd power. Thus, for the same energy and magnetic field electrons radiate 10^{13} more power and with a critical frequency $6\ 10^9$ times higher. Until recently the emission of SR in proton rings has not been of major concern, however, with the advent of the LHC and SSC this situation has changed. Table 2 lists the relevant parameters for some existing and future high energy proton machines.

Table 2
Main parameters for various high energy proton accelerators

Ring	E [TeV]	ρ [m]	B [T]	U_0 [keV]	I_b [mA]	P [kW]	ε_c [eV]
HERA	0.8	584	4.7	0.006	159	0.0009	0.003
Tevatron	1.0	754	4.4	0.011	2.5	0.0003	0.005
LHC	7.7	2568	10.0	10.7	851	9.1	63.7
SSC	20.0	10187	6.6	126	72	8.8	288

It can be seen that there are significant differences in the properties of the SR between the present and future generation of high energy proton machines. The consequences are particularly significant in the case of LHC and SSC since both rings employ superconducting magnets with a cold-bore vacuum tube [39, 40]. The SR power, although modest by electron ring standards, must be absorbed at cryogenic temperatures and represents a significant fraction of the heat input to the cryogenic system. To overcome this problem screens will be employed at a higher temperature than the vacuum pipe, on which the SR power will be absorbed more efficiently. A second problem is the effect on the vacuum pressure. The critical energy of the radiation in the LHC and SSC is sufficiently high to cause photo-desorption of gas molecules. These molecules will then be physisorbed by the screen which acts as a powerful cryopump. After a time a monolayer of adsorbed material can build up, whereupon the thermal vapour pressure of H_2 will increase rapidly leading to a catastrophic pressure rise. Solutions to this problem, involving slots in the shield to pump the desorped gas molecules onto the colder vacuum tube surface, away from the impinging synchrotron radiation, are presently receiving detailed attention [41].

7.2 Modified synchrotron radiation properties

Although the spectrum of radiation emitted by a proton is in general described by the same equations as for an electron, an important difference can arise under certain conditions. In the derivation of section 3 it was assumed implicitly that the magnetic field was constant over the arc length seen by the observer (Fig. 2) i.e. over a distance L_o given by:

$$L_o \simeq \frac{\rho}{\gamma} = \frac{mc}{eB} \tag{52}$$

With a field of 1 T for example this corresponds to a length of 1.7 mm for electrons and 3.1 m for protons. Thus in general magnet lengths exceed the required value for the previous calculation to be valid. It has been shown however that an effect can be produced on the spectrum if at the edge of the magnet the field rises from zero to B, or falls from B to zero, in a distance ΔL that is smaller than L_o [42]. In the case of electrons this condition is not normally met, but in the case of protons a typical magnet edge ($\Delta L \sim 0.1$ m) is usually much smaller than the distance L_o. Since the effect is to shorten the emitted radiation pulse the resulting spectrum extends to higher critical frequency than that corresponding to the central magnet field, ω_c, and is given approximately by:

$$\omega_c' \simeq \frac{L_o}{\Delta L}\,\omega_c \tag{53}$$

This "edge-effect" was observed for the first time on the SPS [43]. At 270 GeV and with a 1.2 T dipole field the standard critical wavelength of 16 μm lies in the infra-red region of the spectrum. The magnet edge, $\Delta L \sim 0.1$ cm, was much shorter than the value of $L_o = 2.5$ m, and so the radiation emitted by the edge of the magnet had a critical wavelength of about 0.6 μm, in the visible range. Later a special undulator magnet, which can be considered to be a series of short magnets with length smaller than L_o, was installed to produce visible radiation from both protons and anti-protons [44]. More recently a visible light beam monitor was also tested in the Tevatron using the edge-effect [45]. Critical frequencies in the LHC and SSC are already sufficiently high that visible radiation will be produced even without the edge-effect.

ACKNOWLEDGEMENT

C.J. Bocchetta is thanked for many helpful suggestions and useful comments during the preparation of this and the following two chapters.

* * *

REFERENCES

[1] A. Liénard, L'Éclairage Électrique 16 (1898) 5.

[2] G.A. Schott, Electromagnetic Radiation, Cambridge University Press, 1912.

[3] D. Iwanenko and I. Pomeranchuk, Phys. Rev. 65 (1944) 343.

[4] J.P. Blewett, Phys. Rev. 69 (1946) 87.

[5] J. Schwinger, Phys. Rev. 70 (1946) 798.

[6] F.R. Elder et. al., Phys. Rev. 71 (1947) 829.

[7] H.C. Pollock, Am. J. Phys. 51 (1983) 278.

[8] J.P. Blewett, Nucl. Instr. Meth. Phys. Res. A266 (1988) 1.

[9] F.R. Elder, R.V. Langmuir and H.C. Pollock, Phys. Rev. 74 (1948) 52.

[10] J. Schwinger, Phys. Rev. 75 (1949) 1912.

[11] D.A. Corson, Phys. Rev. 90 (1953) 748.

[12] D.H. Tomboulian and P.L. Hartman, Phys. Rev. 102 (1956) 1423.

[13] Iu.M. Ado and P.A. Cherenkov, Soviet Physics Doklady 1 (1956) 517.

[14] N.H. Frank, Phys. Rev. 70 (1946) 177.

[15] D. Bohm and L. Foldy, Phys. Rev. 70 (1946) 249.

[16] J. Schwinger, Phys. Rev. 70 (1946) 798.

[17] A.A. Sokolov and J.M. Ternov, J. Exp. Theor. Phys. USSR 25 (1953) 698.
A.A. Sokolov and J.M. Ternov, Soviet Physics JETP 1 (1955) 227.

[18] M. Sands, Phys. Rev. 97 (1955) 470.

[19] A.A. Kolomenski and A.N. Lebedev, CERN Symposium (1956) p. 47.

[20] I.G. Henry, Phys. Rev. 106 (1957) 1057.

[21] F.A. Korolev at. al., Soviet Physics Doklady 6 (1960) 1011; Nuovo Cimento 18 (1960) 1033.

[22] J.D. Jackson, Classical Electrodymanics, Wiley, New York (1962).

[23] H. Bruck, Accélérateurs Circulaires de Particules, Presses Universitaires de France, Paris (1966).

[24] A.A. Sokolov and I.M. Ternov, Synchrotron Radiation, Akadamie-Verlag, Berlin (1968).

[25] G.K. Green, Spectra and Optics of Synchrotron Radiation, Brookhaven National Laboratory, BNL 50522, April 1976.

[26] A. Hofmann, Proc. CERN Accelerator School, Synchrotron Radiation and Free Electron Lasers, CERN 90-03, p. 115.

[27] K.J. Kim, Characteristics of Synchrotron Radiation, AIP Conference Proceedings, 184 vol. 1, AIP, New York (1989) p. 565.

[28] LEP Design Report Vol. II, CERN-LEP/84-01 (1984).

[29] O. Grobner, Proc. CERN Accelerator School, General Accelerator Physics, CERN 85-19, p. 489.

[30] The PETRA Storage Ring group, Proc. 11th Int. Conf. High Energy Accelerators, CERN, July 1980, Birkhaüser Verlag (1980) p. 16.

[31] T. Momose et. al., Proc. 1st European Particle Accelerator Conference, Rome, June 1988, World Scientific (1989) p. 1284.

[32] HERA-Proposal, DESY HERA 81-10, July 1981.

[33] A. Hofmann and F. Meot, Nucl. Instr. Meth. 203 (1982) 483.

[34] V.P. Suller, Proc. CERN Accelerator School, Synchrotron Radiation and Free Electron Lasers, CERN 90-03, p. 74.

[35] V.P. Suller, Proc. 3rd European Particle Accelerator Conference, Berlin, March 1992, Editions Frontieres (1992) p. 77.

[36] F. Ciocci, Proc. 3rd European Particle Accelerator Conference, Berlin, March 1992, Editions Frontieres (1992) p. 86.

[37] W.S. Trzeciak, IEEE Trans. Nucl. Sci. NS-18 (1971) 213.

[38] P. Elleaume, Proc. 1991 US Particle Accelerator Conference, IEEE 91CH3038-7, p. 1083.

[39] W. Chou, Proc. 1991 US Particle Accelerator Conference, IEEE 91CH3038-7, p. 126.

[40] J. Gomez-Goni et. al., Proc. 3rd European Particle Accelerator Conference, Berlin, March 1992, Editions Frontieres (1992) p. 1576.

[41] A.G. Mathewson, these Proceedings.

[42] R. Coisson, Opt. Comm. 22 (1977) 135.

[43] R. Bossart et. al., Nucl. Instr. Meth. 164 (1979) 375.

[44] J. Bosser et. al., J. Physique Lett. 45 (1984) L343.

[45] A.A. Hahn and P. Hurh, Proc. 1991 U.S. Particle Accelerator Conference, IEEE 91CH3038-7, p. 1177.

APPENDIX

PRACTICAL SYNCHROTRON RADIATION FORMULAE

We first consider the most common case of electrons.

Equation (32) gives the energy radiated per unit solid angle per unit frequency interval during the passage of a single particle. In the case of a beam of particles the total energy per second, i.e. the radiated power (in Watts) is proportional to the number of particles that pass the observer per second:

$$\frac{d^2P}{d\Omega\, d\omega} = \frac{d^2W}{d\Omega d\omega}\ \frac{I_b}{e}$$

where I_b is the average beam current in Amps. The frequency interval can be expressed in any desired unit e.g. Hz, Ångstrom, wavenumbers etc. We use here the photon energy (ε), expressed in eV, which in practical units becomes (in Watts/mrad^2/eV):

$$\frac{d^2P}{d\Omega\, d\varepsilon} = 2.124\ 10^{-3}\ E^2\ [\mathrm{GeV}]\ I_b\ [\mathrm{A}] \left(\frac{\varepsilon}{\varepsilon_c}\right)^2 \left(1+\gamma^2\psi^2\right)^2 \left[K_{2/3}^2\left(\xi\right) + \frac{\gamma^2\psi^2}{1+\gamma^2\psi^2}\ K_{1/3}^2\left(\xi\right)\right]$$

where the critical photon energy is given by:

$$\varepsilon_c\ [\mathrm{keV}] = 0.665\ E^2\ [\mathrm{GeV}]\ B[\mathrm{T}] = 2.218\ E^3\ [\mathrm{GeV}]\ /\ \rho$$

and the alternative critical wavelength as:

$$\lambda_c\left[\text{Å}\right] = 18.64\ /\ \left(E^2\ [\mathrm{GeV}]\ B[\mathrm{T}]\right) = 5.589\ \rho\ /\ E^3\ [\mathrm{GeV}]$$

It is also common to express SR intensities in terms of the number of photons per second, obtained by dividing the power in a given frequency interval by the appropriate photon energy $\hbar\omega$. Alternatively the power divided by $\hbar$ gives the number of photons per second per unit *relative* bandwidth:

$$\frac{d^2F}{d\Omega\, d\omega/\omega} = \frac{d^2P}{d\Omega\, d\omega}\ \frac{1}{\hbar}$$

In practical units therefore (photons/s/0.1% bandwidth/mrad^2):

$$\frac{d^2F}{d\Omega\, d\omega\,/\,\omega} = 1.325\ 10^{13}\ E^2\ [\mathrm{GeV}]\ I_b\ [\mathrm{A}] \left(\frac{\varepsilon}{\varepsilon_c}\right)^2 \left(1+\gamma^2\psi^2\right)^2 \left[K_{2/3}^2\left(\xi\right) + \frac{\gamma^2\psi^2}{1+\gamma^2\psi^2}\ K_{1/3}^2\left(\xi\right)\right]$$

and on-axis, ($\psi = 0$):

$$\frac{d^2F}{d\Omega\, d\omega\,/\,\omega} = 1.325\ 10^{13}\ E^2\ [\mathrm{GeV}]\ I_b\ [\mathrm{A}]\ H_2\left(\varepsilon\,/\,\varepsilon_c\right)$$

Integrating over the vertical angle, the spectral distribution per unit horizontal angle becomes (in Watts/mrad/eV):

$$\frac{d^2P}{d\theta\, d\varepsilon} = 6.347\ 10^{-3}\ E\ [\mathrm{GeV}]\ I_b\ [\mathrm{A}]\ S\left(\varepsilon / \varepsilon_c\right)$$

and expressed in terms of photon flux (photons/s/0.1% bandwidth/mrad horizontal):

$$\frac{d^2F}{d\theta\, d\omega / \omega} = 3.96\ 10^{13}\ E\ [\mathrm{GeV}]\ I_b\ [\mathrm{A}]\ S\left(\varepsilon / \varepsilon_c\right)$$

The angular distribution of total power, Eq. (41), becomes (Watts/mrad^2):

$$\frac{dP}{d\Omega} = 5.42\ E^4\ [\mathrm{GeV}]\ B\ [\mathrm{T}]\ I_b[\mathrm{A}]\ \frac{1}{\left(1+\gamma^2\psi^2\right)^{5/2}}\left[1+\frac{5\gamma^2\psi^2}{7\left(1+\gamma^2\psi^2\right)}\right]$$

On-axis therefore the peak power density is given by:

$$\frac{dP}{d\Omega} = 5.42\ E^4\ [\mathrm{GeV}]\ B\ [\mathrm{T}]\ I_b\ [\mathrm{A}] \qquad \mathrm{W/mrad^2}$$

Integrating over vertical angle gives the linear power density:

$$\frac{dP}{d\theta} = 4.22\ E^3\ [\mathrm{GeV}]\ B\ [\mathrm{T}]\ I_b\ [\mathrm{A}] \qquad \mathrm{W/mrad\ horizontal}$$

The formulae above are valid for electrons. In the case of protons the results must be scaled by an appropriate factor α^n where α is the ratio of electron to proton mass i.e. α = 1/1823. Thus, ε_c scales as α^3, λ_c as $1/\alpha^3$, $d^2P/d\Omega d\omega$ and $d^2F/d\Omega(d\omega/\omega)$ as α^2, $d^2P/d\theta d\omega$ and $d^2F/d\theta(d\omega/\omega)$ as α, $dP/d\Omega$ as α^5, $dP/d\theta$ as α^4.